

PLANAR CRACKS IN UNIFORM MOTION UNDER MODE I AND II LOADINGS

P.N.B. ANONGBA

U.F.R. Sciences des Structures de la Matière et de Technologie, Laboratoire de Physique de l'Atmosphère et de Mécanique des Fluides, Université F.H.B. de Cocody, 22 BP 582 Abidjan 22, Côte d'Ivoire

* Correspondance, e-mail : anongba@gmail.com

ABSTRACT

Planar straight-fronted cracks, inside an infinitely extended isotropic elastic medium, whose finite lengths increase at a constant velocity $2v$, are the subject of the present study. The modes J of applied loading ($J = I$ and II) are considered separately. Cracks are represented by continuous distributions of straight edge dislocations J ($J = I$ and II) with Burgers vectors \mathbf{b}_J directed along the applied tension and shear, respectively. Explicit expressions of the elastic fields (displacement and stress) of the crack dislocations J moving uniformly at a velocity v are first given for velocities ranging from zero to values exceeding c_l , the velocity of longitudinal sound waves. Then, crack physical quantities are given, namely the dislocation distribution function D_J , the relative displacement ϕ_J of the faces of the crack, the crack-tip stresses and the crack extension force $G^{(J)}$ per unit length of the crack front. These results cover the velocity range $[0, c_l]$. In mode I loading and in the subsonic velocity regime ($v < c_t$, the velocity of transverse sound wave), $G^{(I)}$ increases continuously with v from the value in the static case $G_0^{(I)} (v = 0)$ to a maximum $G_{\max}^{(I)} \cong 1.32G_0^{(I)}$ at $v = v^{(e)} \cong 0.52 c_t$; then, $G^{(I)}$ decreases rapidly to zero when v tends to c_t . In agreement with experiments, the value $v^{(e)}$ corresponding to the maximum of the crack extension force is identified to the terminal tensile crack velocity, observed in the fracture of brittle materials. No reference is made to the Rayleigh wave velocity c_R . In the transonic speed regime ($c_t < v < c_l$), the crack characteristic functions are identical in form with those of the subsonic regime. However, for $v < c_t\sqrt{2}$, we show that the faces of the crack, separated under load before the extension of the crack, close under motion; this indicates that the crack movement is hindered. for $v > c_t\sqrt{2}$, the motion of the crack is possible. In mode II loading and in the subsonic regime ($v < c_t$), $G^{(II)}$ increases continuously with v (when $v < c_R$) from the value in the static case $G_0^{(II)} (v = 0)$; when

P.N.B. ANONGBA

v approaches c_R , $G^{(II)}$ increases very rapidly. Above c_R ($c_R < v < c_t$), the relative displacement of the faces of the crack, formed under load before crack motion, closes in motion; this indicates that crack motion is impeded. The velocity of uniformly moving cracks is limited by the Rayleigh wave velocity. In the intermediate speed regime ($c_t < v < c_l$), the crack characteristic functions are similar in form to those below c_R . The movement of the crack is possible.

Keywords : *fracture mechanics, linear elasticity, crack propagation and arrest, dislocations, crack extension force.*

RÉSUMÉ

Fissures planes en mouvement uniforme sous la sollicitation des modes I et II

Des fissures planes à front droit, à l'intérieur d'un milieu isotrope, élastique, infiniment étendu, dont les longueurs augmentent à vitesse constante $2v$, font l'objet de la présente étude. Les modes J de charge appliquée ($J = I$ et II) sont considérés séparément. Les fissures sont représentées par des distributions continues de dislocations coins droites J ($J = I$ et II) avec des vecteurs de Burgers b_J dirigés suivant la tension et le cisaillement appliqués, respectivement. Des expressions explicites des champs élastiques (déplacement et contrainte) des dislocations J de fissure en mouvement uniforme de vitesse v sont d'abord données pour des vitesses allant de zéro à des valeurs excédant c_l , la célérité des ondes longitudinales. Ensuite, des grandeurs physiques caractéristiques des fissures sont données, notamment la fonction de distribution D_J des dislocations, le déplacement relatif ϕ_J des lèvres de la fissure, les contraintes en tête de fissure et la force d'extension $G^{(J)}$ de fissure par unité de longueur du front de fissure. Ces résultats couvrent le domaine de vitesse $[0, c_l]$. En mode I de sollicitation et dans le régime de vitesse subsonique ($v < c_t$, la célérité des ondes transversales), $G^{(J)}$ croît continûment avec v à partir de la valeur $G_0^{(I)}$ correspondant au cas statique ($v = 0$) pour atteindre un maximum $G_{\max}^{(I)} \cong 1.32G_0^{(I)}$ à $v = v^{(e)} \cong 0.52 c_t$; puis, $G^{(I)}$ décroît rapidement vers zéro lorsque v s'approche de c_t . En accord avec des expériences, la valeur $v^{(e)}$ correspondant au maximum de la force d'extension de fissure est identifiée à la vitesse terminale des fissures sous tension, observée dans la fissuration des matériaux fragiles. Aucune référence n'est faite à la célérité d'ondes de Rayleigh. Dans le régime de vitesse transsonique ($c_t < v < c_l$), les fonctions caractéristiques de fissure sont identiques en forme à celles du régime subsonique. Cependant, pour $v < c_t\sqrt{2}$, nous montrons que les lèvres de la fissure, écartées sous charge avant le départ de la fissure, tendent à se refermer en cours de mouvement ; ceci suggère que le mouvement est inhibé.

Pour $v > c_t\sqrt{2}$, le mouvement de la fissure devient possible. En mode II de sollicitation et dans le régime de vitesse subsonique ($v < c_t$), $G^{(II)}$ croît continûment avec v (quand $v < c_R$) à partir de la valeur calculée dans le cas statique $G_0^{(II)}(v = 0)$; lorsque v tend vers c_R , $G^{(II)}$ croît beaucoup plus rapidement. Au-dessus de c_R ($c_R < v < c_t$), le déplacement relatif des lèvres de la fissure, formé sous charge avant le départ de la fissure, se referme en cours de mouvement ; ceci indique que le mouvement de la fissure est entravé. La vitesse des fissures en mouvement uniforme est limitée par la vitesse d'ondes de Rayleigh. Dans le régime de vitesse intermédiaire ($c_t < v < c_l$), les fonctions de fissure sont similaires en forme à celles en dessous de c_R . Le mouvement de la fissure devient possible.

Mots-clés : *mécanique de la rupture, élasticité linéaire, propagation et arrêt de fissure, dislocation, force d'extension de fissure.*

I - INTRODUCTION

In several works, we have analysed cracks in elastic solids under different types of applied loading:

- tension, shear and tension + shear in (a) homogeneous media [1 – 7] and (b) bi-materials (interface cracks) [8 - 10],
- compression and flexion [11, 12],
- contact pressure of a cylinder on a flat boundary [13].

The methodology of analysis is invariably the same: the crack is represented by a continuous distribution of infinitesimal dislocations. Explicit expressions of the elastic fields (displacement and stress) of the dislocations are first given; those due to the crack are then obtained by superposition. We consider large cracks corresponding to fracture propagation over macroscopic distances. The methodology is conceptually simple. Mathematically, the main difficulty is the determination of the dislocation elastic fields. The dislocations are rectilinear for planar straight-fronted cracks and sinusoidal for non-planar plane fronted cracks. For an observer in the laboratory reference system, the analysis applies mainly to static cracks under load. It is tempting to extend the analysis to moving cracks with the aim of describing various aspects of the fracture of materials by starting directly with explicit expressions of the dislocation elastic fields. In the present study, one of the simplest movements is analyzed: the uniform rectilinear motion of a planar crack with a straight front. The model is illustrated in **Figure 1**. The medium is isotropic, elastic and infinitely extended, to which is attached a Cartesian system x_i . It consists of a crack in Ox_1x_3 of

finite extension along x_1 with a straight front parallel to x_3 . The crack is under load; initially, it is static and extends from $x_1 = -a$ to a . At a given time taken as $t = 0$ and load σ_{ij}^a , it starts moving at constant velocity v . Its extension after time interval t is given by $|x_1| \leq c = a + vt$. We shall consider separately uniform tension σ_{22}^a (mode I) and shear σ_{21}^a (mode II) applied at infinity.

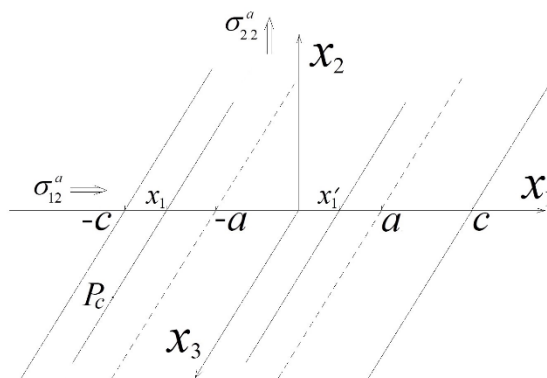


Figure 1 : Planar straight-fronted crack in uniform motion at velocity v from initial spreading $|x_1| \leq a$ ($t = 0$) to $|x_1| \leq c = a + vt$ after time interval t . Uniform applied stresses at infinity σ_{22}^a (mode I loading) and σ_{21}^a (mode II) are considered separately; see the text

The crack is represented by a continuous distribution of infinitesimal dislocations parallel to x_3 with Burgers vectors $\vec{b}_I = (0, b, 0)$ for the mode I loading and $\vec{b}_{II} = (b, 0, 0)$ for mode II. Dislocation distributions D_J ($J = I$ and II) are defined such that $D_J(x_1') dx_1'$ represents the number of dislocations J in the infinitesimal x_1 - interval dx_1' located about the x_1 - spatial position x_1' . In the Section 2 (Methodology), the method adopted to calculate the dislocation elastic fields (displacement and stress) is presented first; then, the crack analysis is explained in order to reach physical quantities such as D_J , relative displacement ϕ_j of the faces of the crack, crack-tip stress $\bar{\sigma}_{ij}^{(J)}$ and crack extension force $G^{(J)}$. The results are collected in Section 3. Section 4 and 5 are devoted to the discussion and conclusion, respectively.

II - METHODOLOGY

II-1. Elastic fields of uniformly moving straight dislocations

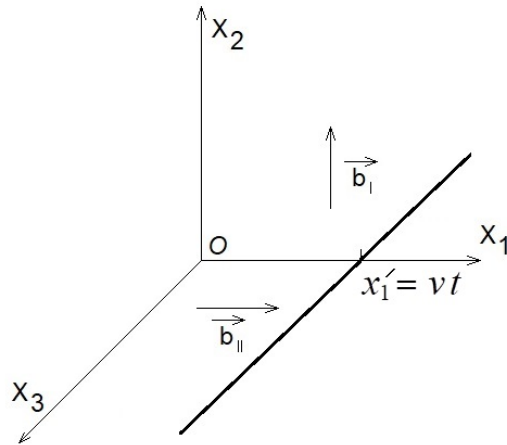


Figure 2 : *Infinitely long straight dislocation J parallel to x_3 travelling uniformly at constant speed v in the x_1 - direction, with Burgers vector \vec{b}_J directed along x_1 ($J = II$) or x_2 ($J = I$)*

We are concerned with the determination of the displacement and stress fields ($\vec{u}^{(J)}$, $(\sigma)^{(J)}$) of straight edges parallel to x_3 in uniform motion along x_1 in the Ox_1x_3 – plane (**Figure 2**). The two types ($J = I$ and II) of dislocation considered have Burgers vectors \vec{b}_J parallel to x_2 and x_1 , respectively. The dislocations are located at the origin when $t = 0$ and at spatial x_1 - position $x_1' = vt$ after incremental time t . We shall make use of the displacement $u_m(\vec{x}, t)$ (see (2) below) to a prescribed plastic distortion $\beta_{ij}^*(\vec{x}, t)$ given as a periodic function of coordinates and time

$$\beta_{ij}^* = \bar{\beta}_{ij}^* e^{i(\omega t + \vec{k} \cdot \vec{x})} \tag{1}$$

where $\vec{k} \cdot \vec{x} = k_1 x_1 + k_2 x_2 + k_3 x_3$; in the above expression, k_i and ω are arbitrary constants and $\bar{\beta}_{ij}^*$ are arbitrary functions of k_i and ω . Mura [18, 19] has shown the associated displacement component to be

$$u_m(\vec{x}, t) = -ik_l C_{klji} L_{mk} \bar{\beta}_{ij}^* e^{i(\omega t + \vec{k} \cdot \vec{x})}. \tag{2}$$

For isotropic material,

$$L_{mk} = \frac{\delta_{km} \left((\lambda + 2\mu)k^2 - \rho\omega^2 \right) - k_k k_m (\lambda + \mu)}{\left(\mu k^2 - \rho\omega^2 \right) \left((\lambda + 2\mu)k^2 - \rho\omega^2 \right)} \quad (3)$$

where $k^2 = k_1^2 + k_2^2 + k_3^2$ and

$$C_{klji} = \lambda \delta_{kl} \delta_{ji} + \mu \delta_{kj} \delta_{li} + \mu \delta_{ki} \delta_{lj}, \quad (4)$$

δ_{ij} being the Kronecker delta and λ and μ are Lamé's constants. The plastic distortions $\beta_{ij}^{*(J)}(\vec{x}, t)$ associated to the dislocations J ($J = I$ and II), **Figure 2**, are

$$\begin{aligned} \beta_{12}^{*(I)} \delta_{II} + \beta_{21}^{*(II)} \delta_{III} &= b \left[\delta_{II} \delta(x_1 - vt) H(x_2) + \delta_{III} \delta(x_2) H(-(x_1 - vt)) \right] \\ &= \int_{-\infty}^{\infty} \int_{-\infty}^{\infty} \bar{\beta}^{*(J)} e^{i(k_1 y_1 + k_2 x_2)} dk_1 dk_2 \end{aligned} \quad (5)$$

with $\bar{\beta}^{*(J)} = -(ib / 4\pi^2) (\delta_{II} / k_2 - \delta_{III} / k_1)$, the other components of the plastic distortions are zero; δ and H are the Dirac delta and Heaviside step functions, respectively; $y_1 = x_1 - vt$. $\beta_{ij}^{*(J)}$ (5) appear to be superpositions of wave expressions of the form β_{ij}^* (1). Therefore, the associated displacements $\vec{u}^{(J)}$ are similar superpositions of the displacement \vec{u} (2). We may write

$$u_m^{(J)}(\vec{x}, t) = \int_{-\infty}^{\infty} \int_{-\infty}^{\infty} -ik_l C_{kl12} L_{mk} \bar{\beta}^{*(J)} e^{i(k_1 y_1 + k_2 x_2)} dk_1 dk_2. \quad (6)$$

Useful relations are

$$\frac{\partial}{\partial x_1} u_m^{(II)} = \frac{\partial}{\partial y_1} u_m^{(II)} = -\frac{\partial}{\partial x_2} u_m^{(I)}. \quad (7)$$

The stress fields $(\sigma)^{(J)}$ can be obtained by differentiating the displacements (6). Our calculation results are displayed in Section 3.

II-2. Crack analysis

The analysis methodology consists in representing the crack (**Figure 1**) in mode J ($J = I$ and II) by a continuous distribution of dislocations J as introduced in Section 1. To obtain the dislocation distribution functions D_J at equilibrium, one may ask that the faces of the crack be traction free, or that the total force along x_1 at any point P_C of the crack dislocations be zero. The following equations are reached

$$\delta_{II}\sigma_{22}^a + \delta_{III}\sigma_{21}^a + \int_{-c}^c (\delta_{II}\sigma_{22}^{(I)} + \delta_{III}\sigma_{21}^{(II)})D_J(x_1')dx_1' = 0. \tag{8}$$

$\sigma_{22}^{(I)}$ and $\sigma_{21}^{(II)}$ are the stresses at P_C due to the dislocations I and II located at x_1' along the x_1 direction. (8) gives two integral equations, the resolutions of which, yield the D_J . The relative displacement of the faces of the crack are obtained by integration from the relation $d\phi_J = -bD_J(x_1')dx_1'$:

$$\phi_J(x_1) = \int_{x_1}^c bD_J(x_1')dx_1', \quad |x_1| \leq c. \tag{9}$$

The total stress $(\bar{\sigma})^{(J)}$ at arbitrary position $P(x_1, x_2, x_3)$ in the fractured medium is

$$\bar{\sigma}_{ij}^{(J)}(P) = \sigma_{ij}^{(J)a} + \int_{-c}^c \sigma_{ij}^{(J)}(x_1 - x_1', x_2, x_3)D_J(x_1')dx_1'; \tag{10}$$

$\sigma_{ij}^{(J)a}$ are zero except $\sigma_{22}^{(I)a} = \sigma_{22}^a$ and $\sigma_{21}^{(II)a} = \sigma_{21}^a$; from (10), one can obtain the crack-tip stresses. The crack extension force keeps its definition and is calculated in the same way as in the absolute reference frame of the laboratory on a quasi-static crack under load (see [20]). To be convinced, it suffices to place oneself in the inertial reference frame traveling with the crack front; the laws of movement remain unchanged in any inertial reference frame. The elastic fields are seen to depend on the spatial coordinates y_1 and x_2 only. Our definition of the crack extension force is stated as follows: “A crack of length l is considered at equilibrium under load (use **Figure 1** for illustration). Then, this crack grows steadily over a short distance from one of its ends while the other end remains fixed. A work associated with a newly created surface element Δs is then calculated, which is the product of the elastic force on the element (just before the motion of the crack tip) by the relative displacement of the faces of the newly created crack through Δs . This energy is then divided by Δs ; the limit $G^{(J)}$ taken by the ratio of that energy divided by Δs when the latter tends to zero is by definition the crack extension force per unit length of the crack front at the point P ahead of the crack-tip where Δs is located.”. To account for the energy released when both tips of the crack move, we multiply the crack extension force by 2.

III - RESULTS

III-1. Elastic fields of straight edges in uniform motion

III-1-1. Subsonic velocity regime ($v < c_t$)

This regime corresponds to $v < c_t$ where c_t is the velocity of transverse sound wave. We have

$$u_m^{(j)} = \frac{b}{2\pi\tilde{v}_t^2} \left(\ln(y_1^2 + P_t^2 x_2^2) [\delta_{JI} \delta_{m1} / P_t + \delta_{JII} \delta_{m2} P_t] - (P_{2t}^2 / P_t) \ln(y_1^2 + P_t^2 x_2^2) \right. \\ \left. \times [\delta_{JI} \delta_{m1} + \delta_{JII} \delta_{m2}] + 2 \tan^{-1}(y_1 / x_2 P_t) [\delta_{JI} \delta_{m2} - \delta_{JII} \delta_{m1}] \right. \\ \left. + 2P_{2t}^2 \tan^{-1}(y_1 / x_2 P_t) [\delta_{JII} \delta_{m1} - \delta_{JI} \delta_{m2} / P_t^2] \right); \quad (11)$$

$$\tilde{v}_t = v / c_t, \quad P_t^2 = 1 - \tilde{v}_t^2, \quad P_{2t}^2 = 1 - \tilde{v}_t^2 / 2;$$

$$\tilde{v}_l = v / c_l, \quad P_l^2 = 1 - \tilde{v}_l^2;$$

the subscript m takes the values 1 and 2 and c_l is the velocity of longitudinal sound wave. In the logarithm, x_2 and y_1 stand for dimensionless variables. Other displacement components are zero. Associated stresses involved in crack analyses are

$$\delta_{JI} \sigma_{22}^{(I)} + \delta_{JII} \sigma_{21}^{(II)} = \frac{2\mu b}{\pi\tilde{v}_t^2} y_1 \left(\frac{P_{2t}^2}{y_1^2 + P_t^2 x_2^2} \left[\frac{\delta_{JI}}{P_t} - \frac{P_{2t}^2 \delta_{JII}}{P_t} \right] \right. \\ \left. + \frac{1}{y_1^2 + P_t^2 x_2^2} \left[\delta_{JII} P_t - \delta_{JI} \frac{P_{2t}^2}{P_t} \right] \right), \\ \sigma_{21}^{(I)} = \frac{2\mu b}{\pi\tilde{v}_t^2} x_2 \left(\frac{P_l}{y_1^2 + P_l^2 x_2^2} - \frac{P_{2t}^4}{P_t (y_1^2 + P_t^2 x_2^2)} \right). \quad (12)$$

III-1-2. Intermediate (transonic) velocity regime ($c_t < v < c_l$)

We obtain for the displacements

$$u_1^{(I)} = \frac{b}{2\pi\tilde{v}_t^2} \left(\frac{1}{P_t} \ln(y_1^2 + P_t^2 x_2^2) + \frac{2 - \tilde{v}_t^2}{\sqrt{\tilde{v}_t^2 - 1}} H_1 \right), \\ u_2^{(I)} = -\frac{b}{2\pi\tilde{v}_t^2} \left(2 \tan^{-1}(P_t x_2 / y_1) + \frac{2 - \tilde{v}_t^2}{\tilde{v}_t^2 - 1} \operatorname{sgn}(y_1) \operatorname{sgn}(x_2) H_2 \right); \quad (13)$$

$$u_1^{(II)} = \frac{b}{2\pi\tilde{\nu}_t^2} \left(2 \tan^{-1} (P_t x_2 / y_1) + (2 - \tilde{\nu}_t^2) \operatorname{sgn}(y_1) \operatorname{sgn}(x_2) H_1 \right),$$

$$u_2^{(II)} = \frac{b}{2\pi\tilde{\nu}_t^2} \left(P_t \ln (y_1^2 + P_t^2 x_2^2) + \frac{2 - \tilde{\nu}_t^2}{\sqrt{\tilde{\nu}_t^2 - 1}} H_1 \right); \tag{14}$$

$\operatorname{sgn}(x_i) = |x_i| / x_i$. H_1 and H_2 take values according to spatial regions as

- a) $\frac{|y_1|}{\sqrt{\tilde{\nu}_t^2 - 1}} > |x_2| \geq 0$: $H_1 = \pi/2$ and $H_2 = 0$,
 - b) $\frac{|y_1|}{\sqrt{\tilde{\nu}_t^2 - 1}} = |x_2| > 0$: $H_1 = \pi/4 = H_2$,
 - c) $|x_2| > \frac{|y_1|}{\sqrt{\tilde{\nu}_t^2 - 1}} \geq 0$: $H_1 = 0$ and $H_2 = \pi/2$.
- (15)

These regions are illustrated in the plot of the relation $|x_2| = |y_1| / \sqrt{\tilde{\nu}_t^2 - 1}$ in **Figure 3**. Associated stresses are

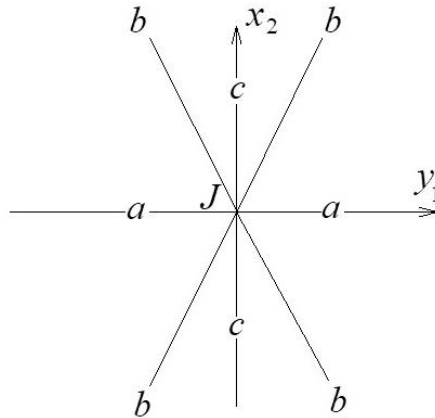


Figure 3 : Plot of the relation $|x_2| = |y_1| / \sqrt{\tilde{\nu}_t^2 - 1}$ for $\sqrt{\tilde{\nu}_t^2 - 1} = 1/2$ at the dislocation J location

$$\begin{aligned}
\sigma_{22}^{(I)} &= \frac{\mu b (\tilde{v}_t^2 - 2)}{\pi \tilde{v}_t^2} \left(\frac{y_1}{P_l (y_1^2 + P_l^2 x_2^2)} + \frac{\pi}{2\sqrt{\tilde{v}_t^2 - 1}} \right. \\
&\times \operatorname{sgn}(y_1) \left[\delta(|x_2| \sqrt{\tilde{v}_t^2 - 1} + |y_1|) + \delta(|x_2| \sqrt{\tilde{v}_t^2 - 1} - |y_1|) \right] \Big), \\
\sigma_{21}^{(II)} &= \frac{\mu b}{\pi \tilde{v}_t^2} \left(\frac{2P_l y_1}{y_1^2 + P_l^2 x_2^2} + \frac{\pi(2 - \tilde{v}_t^2)}{4\sqrt{\tilde{v}_t^2 - 1}} \right. \\
&\times \operatorname{sgn}(y_1) \left[\tilde{v}_t^2 \delta(|x_2| \sqrt{\tilde{v}_t^2 - 1} + |y_1|) + (2 - \tilde{v}_t^2) \delta(|x_2| \sqrt{\tilde{v}_t^2 - 1} - |y_1|) \right] \Big). \quad (16)
\end{aligned}$$

III-1-3. Supersonic velocity regime ($c_l < v$)

We restrict ourselves to the dislocation I only.

$$\begin{aligned}
u_1^{(I)} &= \frac{b}{2\pi \tilde{v}_t^2} \left(\frac{2 - \tilde{v}_t^2}{\sqrt{\tilde{v}_t^2 - 1}} H_1 - \frac{2}{\sqrt{\tilde{v}_t^2 - 1}} H_3 \right), \\
u_2^{(I)} &= \frac{b}{2\pi \tilde{v}_t^2} \operatorname{sgn}(y_1) \operatorname{sgn}(x_2) \left(\frac{\tilde{v}_t^2 - 2}{\sqrt{\tilde{v}_t^2 - 1}} H_2 - 2H_4 \right); \quad (17)
\end{aligned}$$

H_3 and H_4 take constant values according to regions as

$$\begin{aligned}
\text{a) } & \frac{|y_1|}{\sqrt{\tilde{v}_t^2 - 1}} > |x_2| \geq 0: \quad H_3 = \pi/2 \text{ and } H_4 = 0, \\
\text{b) } & \frac{|y_1|}{\sqrt{\tilde{v}_t^2 - 1}} = |x_2| > 0: \quad H_3 = \pi/4 = H_4, \\
\text{c) } & |x_2| > \frac{|y_1|}{\sqrt{\tilde{v}_t^2 - 1}} \geq 0: \quad H_3 = 0 \text{ and } H_4 = \pi/2. \quad (18)
\end{aligned}$$

III-1-4. Special velocities ($v = c_t$ and $v = c_l$)

For $v = c_t$:

$$\begin{aligned}
u_1^{(I)} &= \frac{b}{2\pi} \left(\frac{1}{\sqrt{1 - c_*^2}} \ln(y_1^2 + (1 - c_*^2)x_2^2) - \pi|x_2| \delta(y_1) \right), \\
u_2^{(I)} &= -\frac{b}{\pi} \tan^{-1} \left(\sqrt{1 - c_*^2} \frac{x_2}{y_1} \right); \quad (19)
\end{aligned}$$

$$u_1^{(II)} = \frac{b}{\pi} \tan^{-1} \left(\sqrt{1-c_*^2} \frac{x_2}{y_1} \right) - bH(x_2)H(y_1),$$

$$u_2^{(II)} = \frac{b}{2\pi} \left(\sqrt{1-c_*^2} \ln \left(y_1^2 + (1-c_*^2)x_2^2 \right) - \pi|x_2|\delta(y_1) \right); \tag{20}$$

$c_* = c_l / c_l$, $|x_2|$ is dimensionless.

$$\sigma_{22}^{(I)} = -\frac{\mu b}{\pi \sqrt{1-c_*^2}} \frac{y_1}{y_1^2 + (1-c_*^2)x_2^2},$$

$$\sigma_{21}^{(II)} = \frac{2\mu b \sqrt{1-c_*^2}}{\pi} \frac{y_1}{y_1^2 + (1-c_*^2)x_2^2} - \mu b \delta(x_2)H(y_1). \tag{21}$$

For $v = c_l$: we give the displacement for the dislocation I only

$$u_1^{(I)} = -\frac{bc_*^2}{2\pi} \left(\frac{c_*^{-2} - 2}{\sqrt{c_*^{-2} - 1}} H_5 - 2\pi|x_2|\delta(y_1) \right),$$

$$u_2^{(I)} = \frac{b(1-2c_*^2)}{2\pi(c_*^{-2} - 1)} \text{sgn}(y_1) \text{sgn}(x_2)H_6; \tag{22}$$

H_5 and H_6 are constants in different domains :

- a) $\frac{|y_1|}{\sqrt{c_*^{-2} - 1}} > |x_2| \geq 0$: $H_5 = \pi/2$ and $H_6 = 0$,
- b) $\frac{|y_1|}{\sqrt{c_*^{-2} - 1}} = |x_2| > 0$: $H_5 = \pi/4 = H_6$,
- c) $|x_2| > \frac{|y_1|}{\sqrt{c_*^{-2} - 1}} \geq 0$: $H_5 = 0$ and $H_6 = \pi/2$. (23)

III-2. Moving cracks in mode I loading

III-2-1. Subsonic velocity regime ($v < c_l$)

The dislocation distribution D_J is given by (8) making use of (12). We obtain

$$D_I(x_1) = \frac{\sigma_{22}^a}{\pi C_1^{(I)}} \frac{x_1}{\sqrt{c^2 - x_1^2}} \quad (|x_1| < c = a + vt); \tag{24}$$

$$C_1^{(I)} = \frac{\mu b(2 - \tilde{v}_l^2)}{\pi \tilde{v}_l^2} \left(\frac{1}{P_t} - \frac{1}{P_l} \right). \tag{25}$$

The relative displacement of the faces of the crack from (9) is :

$$\phi_l(x_1) = \frac{b\sigma_{22}^a}{\pi C_1^{(l)}} \sqrt{c^2 - x_1^2} . \quad (26)$$

We use (10) and (12) to calculate the total stress $\bar{\sigma}_{22}^{(l)}$ ahead of the crack tip at $x_1 = c$; substituting $x_1 = c + s$, $0 < s \ll c$, we obtain after integration

$$\bar{\sigma}_{22}^{(l)}(s) = \frac{K_I}{\sqrt{2\pi}} \frac{1}{\sqrt{s}} ; \quad (27)$$

$K_I = \sigma_{22}^a \sqrt{\pi c}$. The crack extension force $G^{(l)}$ per unit edge length as defined in Section 2.2 is

$$G^{(l)} = \frac{bK_I^2}{4\pi C_1^{(l)}} . \quad (28)$$

At $t=0$ and $\nu=0$, $G^{(l)}$ reduces to

$$G_0^{(l)} = \frac{bK_I^2(0)}{4\pi C_0} \quad (29)$$

where $C_0 = \mu b / 2\pi(1-\nu)$ and $K_I(0) = \sigma_{22}^a \sqrt{\pi a}$. We can write $(c-a)/a = \tilde{\nu}_t c_t t / a \equiv \tilde{\nu}_t \tilde{d}_t$; then, the normalized quantity $\tilde{G}^{(l)} = G^{(l)} / G_0^{(l)}$ is reported in **Figure 4** as a function of $\tilde{\nu}_t$ for $\tilde{d}_t = 1$, in other words, when a transverse sound wave emitted at the tip of the crack of length $2a$ travelled a distance equal to half the initial crack length. $\tilde{G}^{(l)}$ increases with $\tilde{\nu}_t$ from the value 1 ($\tilde{\nu}_t = 0$) up to a maximum $\tilde{G}_{\max}^{(l)} \cong 1.32$ located at about $\tilde{\nu}_t^{(e)} = 0.52$; then it decreases to zero as $\tilde{\nu}_t$ tends to 1. $\tilde{G}^{(l)}$ is continuous. The condition for the maximum for $\tilde{G}^{(l)}$ with respect to $\tilde{\nu}_t$ is given by $\partial \tilde{G}^{(l)} / \partial \tilde{\nu}_t = 0$ and this is satisfied when

$$(1 + \tilde{d}_t \tilde{\nu}_t) \tilde{\nu}_t^2 (2 - \tilde{\nu}_t^2) P_t P_l (P_t c_*^2 - P_l) + (P_l - P_t) \left\{ P_t^2 P_l^2 \tilde{\nu}_t (2\tilde{d}_t + \tilde{\nu}_t) + (1 + \tilde{d}_t \tilde{\nu}_t) \right. \\ \left. \times \left[-P_t^2 P_l^2 \tilde{\nu}_t^2 + 4P_t^2 P_l^2 - 4P_l^2 \tilde{\nu}_t^2 + 2(1 - c_*^2) \tilde{\nu}_t^2 + 2P_t^2 \tilde{\nu}_t^4 - (1 - c_*^2) \tilde{\nu}_t^4 \right] \right\} = 0 . \quad (30)$$

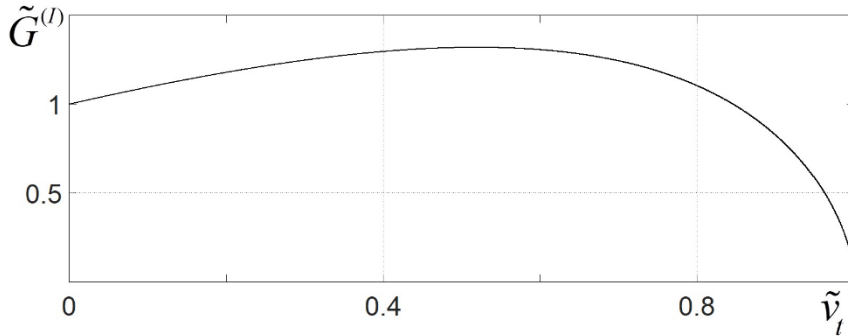


Figure 4 : Normalized crack extension force $\tilde{G}^{(I)} = G^{(I)} / G_0^{(I)}$ (28, 29) versus $\tilde{v}_t = v / c_t$ in subsonic velocity regime $0 \leq \tilde{v}_t \equiv v / c_t < 1$. The curve corresponds to $\tilde{d}_t \equiv c_t t / a = 1$; $\nu = 1/3$

III-2-2. Intermediate velocity regime ($c_t < v < c_l$)

The relation (8) reads

$$\sigma_{22}^a + \int_{-c}^c \sigma_{22}^{(I)}(x_1 - x_1', x_2 = 0, x_3) D_I(x_1') dx_1' = 0$$

where with (16)

$$\sigma_{22}^{(I)}(x_1 - x_1', x_2 = 0, x_3) = \frac{C_2^{(I)}}{x_1 - x_1'} + \frac{\mu b(\tilde{v}_t^2 - 2)}{\tilde{v}_t^2 \sqrt{\tilde{v}_t^2 - 1}} \operatorname{sgn}(x_1 - x_1') \delta(x_1 - x_1');$$

$$C_2^{(I)} = \frac{\mu b(\tilde{v}_t^2 - 2c_*^2)}{\pi \tilde{v}_t^2 \sqrt{1 - \tilde{v}_t^2}}. \tag{31}$$

For $\tilde{v}_t^2 = 2$, $\sigma_{22}^{(I)}$ (16) is identically zero, not only on the fracture surface, but everywhere in the fractured medium. Under such conditions, the condition (8) gives no information on D_I and cannot be satisfied when $\sigma_{22}^a \neq 0$, suggesting that no uniform motion is possible under an applied tension stress. Now, assuming $\tilde{v}_t^2 \neq 2$, (8) becomes

$$\sigma_{22}^a + C_2^{(I)} \int_{-c}^c \frac{D_I(x_1') dx_1'}{x_1 - x_1'} + \frac{\mu b(\tilde{v}_t^2 - 2)}{\tilde{v}_t^2 \sqrt{\tilde{v}_t^2 - 1}} \int_{-c}^c \operatorname{sgn}(x_1 - x_1') \delta(x_1 - x_1') D_I(x_1') dx_1' = 0. \tag{32}$$

(32) differs from the familiar form corresponding to a static crack by the third integral term with the Dirac delta function δ . We suggest that this term is zero

as follows. For $x_1 \neq x_1'$, it is zero; about x_1 , the integral may be written ($0 < \varepsilon$ small real number)

$$\int_{x_1-\varepsilon}^{x_1+\varepsilon} \text{sgn}(x_1 - x_1') \delta(x_1 - x_1') D_I(x_1') dx_1' = D_I(x_1) \int_{-\varepsilon}^{\varepsilon} \text{sgn}(y) \delta(y) dy = 0, \quad (33)$$

because $\text{sgn}(y)\delta(y)$ is odd function. The usual form is recovered,

$$\sigma_{22}^a + C_2^{(I)} \int_{-c}^c \frac{D_I(x_1')}{x_1 - x_1'} dx_1' = 0. \quad (\tilde{v}_l^2 \neq 2) \quad (34)$$

This leads to familiar relations (24), (26) and (27) in which $C_1^{(I)}$ (25) is replaced by $C_2^{(I)}$ (31). It is tempting to include the crack extension form (28) as an indicative estimate, but this not clearly established. The results are collected:

$$D_I(x_1) = \frac{\sigma_{22}^a}{\pi C_2^{(I)}} \frac{x_1}{\sqrt{c^2 - x_1^2}}; \quad \phi_I(x_1) = \frac{b\sigma_{22}^a}{\pi C_2^{(I)}} \sqrt{c^2 - x_1^2}; \quad G^{(I)} = \frac{bK_I^2}{4\pi C_2^{(I)}}. \quad (35)$$

Figure 5 reports $\mu b / \pi C_2^{(I)}$ (31) as a function of $\tilde{v}_l = v / c_l$. This quantity is negative and decreases with \tilde{v}_l for $\tilde{v}_l < c_* \sqrt{2}$; it is positive above $\tilde{v}_l = c_* \sqrt{2}$ and decreasing with \tilde{v}_l . The observed discontinuity is at $\tilde{v}_l = c_* \sqrt{2}$. We stress that a similar analysis can be performed when $v = c_l$ starting from (34) with $C_2^{(I)}(v = c_l)$ given by (31).

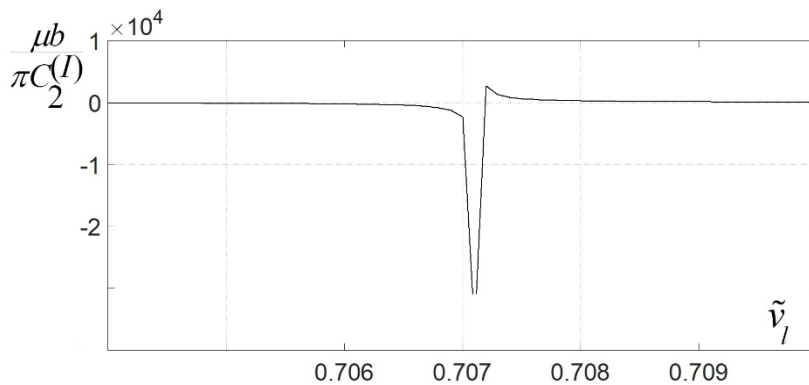


Figure 5 : Quantity $\mu b / \pi C_2^{(I)}$ (31) as a function of $\tilde{v}_l = v / c_l$ in intermediate velocity regime $c_* < \tilde{v}_l < 1$; $c_* = c_l / c_l, v = 1/3$

III-3. Moving cracks in mode II loading

III-3-1. Subsonic velocity regime ($v < c_t$)

The condition (8) becomes

$$\sigma_{21}^a + \int_{-c}^c \sigma_{21}^{(I)}(x_1 - x_1', 0, x_3) D_{II}(x_1') dx_1' = 0$$

where with (16)

$$\begin{aligned} \sigma_{21}^{(II)} &= \frac{C_1^{(II)}}{x_1 - x_1'}; \\ C_1^{(II)} &= \frac{2\mu b(P_t P_l - P_{2t}^4)}{\pi \tilde{v}_t^2 P_t}. \end{aligned} \tag{36}$$

Defining $R_w \equiv P_t P_l - P_{2t}^4$, $C_1^{(II)}$ cancels under the condition $R_w = 0$. This condition can be managed to read

$$\tilde{v}_t^6 - 8\tilde{v}_t^4 + 8\tilde{v}_t^2(3 - 2c_*^2) - 16(1 - c_*^2) = 0. \tag{37}$$

This equation determines Rayleigh wave speed [21]. Hence, a crack dislocation II travelling at the Rayleigh wave speed c_R produces zero stress $\sigma_{21}^{(II)}$ on the $x_2 = 0$ fracture plane. The equilibrium condition (8) can't be fulfilled for $\sigma_{21}^a \neq 0$ suggesting no steady motion under such conditions. Except for the Rayleigh wave speed, we obtain similarly as for the mode I loading

$$\begin{aligned} D_{II}(x_1) &= \frac{\sigma_{21}^a}{\pi C_1^{(II)}} \frac{x_1}{\sqrt{c^2 - x_1^2}}, \quad \phi_{II}(x_1) = \frac{b\sigma_{21}^a}{\pi C_1^{(II)}} \sqrt{c^2 - x_1^2}; \\ \bar{\sigma}_{21}^{(II)}(s) &= \frac{K_{II}}{\sqrt{2\pi}} \frac{1}{\sqrt{s}}, \quad K_{II} = \sigma_{21}^a \sqrt{\pi c}; \\ G^{(II)} &= \frac{bK_{II}^2}{4\pi C_1^{(II)}}, \quad G_0^{(II)} \equiv G^{(II)}(v=0) = \frac{bK_{II}^2(0)}{4\pi C_0}, \quad K_{II}(0) = \sigma_{21}^a \sqrt{\pi a}. \end{aligned} \tag{38}$$

The reduced quantity $\tilde{G}^{(II)} = G^{(II)} / G_0^{(II)}$ is reported in **Figure 6** as a function of \tilde{v}_t for $\tilde{d}_t = 1$.

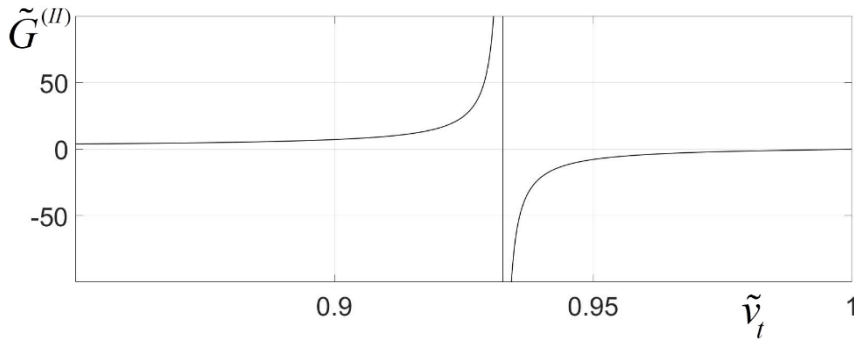


Figure 6 : Reduced crack extension force $\tilde{G}^{(II)} = G^{(II)} / G_0^{(II)}$ (38) versus \tilde{v}_t in subsonic velocity regime. The curve corresponds to $\tilde{d}_t = 1$; $\nu = 1/3$. A vertical asymptote is observed at the Rayleigh wave speed c_R

$\tilde{G}^{(II)}$ increases continuously with \tilde{v}_t (below the Rayleigh wave speed) from the value 1 ($\tilde{v}_t = 0$); the increase is very pronounced when one approaches c_R . Above c_R , $\tilde{G}^{(II)}$ is negative and increases to zero with \tilde{v}_t .

III-3-2. Intermediate velocity regime ($c_t < v < c_l$)

Similarly, as for the corresponding mode I case, it may be written from condition (8)

$$\begin{aligned} \sigma_{21}^a + \int_{-c}^c \sigma_{21}^{(II)}(x_1 - x_1', 0, x_3) D_{II}(x_1') dx_1' &= 0; \\ \sigma_{21}^{(II)} &= \frac{C_2^{(II)}}{x_1 - x_1'} + C_3^{(II)} \operatorname{sgn}(x_1 - x_1') \delta(x_1 - x_1'); \\ C_2^{(II)} &= \frac{2\mu b c_*^2 \sqrt{1 - \tilde{v}_t^2}}{\pi \tilde{v}_t^2}, \quad C_3^{(II)} = \frac{\mu b (2 - \tilde{v}_t^2)}{\pi \tilde{v}_t^2 \sqrt{\tilde{v}_t^2 - 1}}. \end{aligned} \quad (39)$$

Then, follows the integral equation for D_{II}

$$\sigma_{21}^a + C_2^{(II)} \int_{-c}^c \frac{D_{II}(x_1') dx_1'}{x_1 - x_1'} + C_3^{(II)} \int_{-c}^c \operatorname{sgn}(x_1 - x_1') \delta(x_1 - x_1') D_{II}(x_1') dx_1' = 0. \quad (40)$$

The third term with $C_3^{(II)}$ cancels for $\tilde{v}_t^2 = 2$ but as shown for the similar mode I equation (32), this term cancels whatever the velocity v . Again, the familiar form is reached

$$\sigma_{21}^a + C_2^{(II)} \int_{-c}^c \frac{D_{II}(x_1')}{x_1 - x_1'} dx_1' = 0; \tag{41}$$

with associated quantities as in (38). For $\tilde{v}_l^2 = 2$, the crack extension force is given by the form $G^{(II)}$ (38) in which $C_1^{(II)}$ is replaced by $C_2^{(II)}$ (39). On **Figure 7** is reported $2\mu bc_*^2 / \pi C_2^{(II)}$ as a function of \tilde{v}_l . It increases continuously with \tilde{v}_l . A vertical asymptote is present at $\tilde{v}_l = 1$.

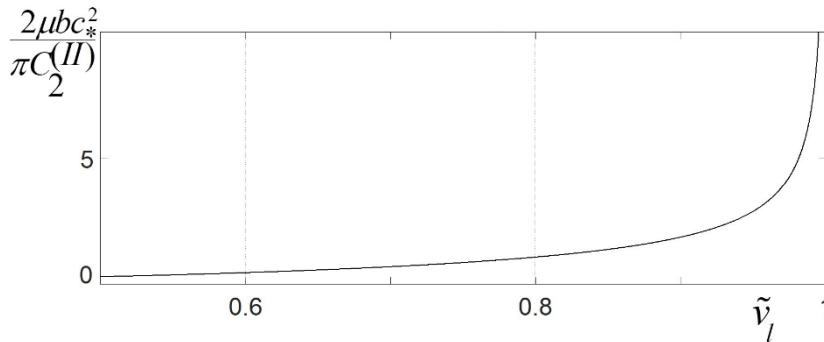


Figure 7 : Quantity $2\mu bc_*^2 / \pi C_2^{(II)}$ (39) as a function of \tilde{v}_l in intermediate velocity regime $c_* < \tilde{v}_l < 1$; mode II loading, $\nu = 1/3$

IV - DISCUSSION

IV-1. Dislocations

The determination of the elastic fields of dislocations in motion may be performed by two general methods called “Method of Fourier series or integrals” and “Method of Green’s functions” in review works by Mura [18, 19]. The first method, especially powerful for many cases, is the one adopted in the present study (Section 2.1); it has been used to obtain the elastic fields of a dislocation oscillating in the form of a standing wave [2], for example. Earlier studies of dislocations in uniform motion are referenced by Eshelby [22]. The results listed in Section 3.1 cover the broad values of the dislocation velocity, from subsonic ($v < c_l$) to supersonic ($c_l < v$). A remarkable difference of the elastic fields of moving dislocations, as compared to static ones, is the presence in their stress fields of singularities of the type of the Dirac delta function, along lines crossing transversely the dislocation, when the velocity v is larger than the velocity of transverse sound wave; these lines are illustrated in **Figure 3**. Another observation is that the elastic fields, measured by an observer in an

inertial reference frame moving with the dislocation, are like those of a static dislocation in the laboratory, particularly in the subsonic regime. This allows to describe static and uniformly moving cracks in a similar way.

IV-2. Mode I loaded cracks

In the subsonic regime, the crack-tip characteristic functions are similar in form with those of a static crack. They depend on v through $C_1^{(J)}$ ($J= I$ and II) and $c = a + vt$; when $v = 0$ and $vt = 0$, the static case is recovered. A special behaviour observed by experimentalists is as follows: an initial static crack ($|x_1| \leq a$, when using **Figure 1** as illustration) is under load in tension (mode I); at a given time taken as $t = 0$, it starts to move. It is found experimentally that the crack velocity increases gradually to a constant terminal velocity. This property of tensile cracks is captured on micrographs by Kerkhof and Richter [23], **Figure 8**.

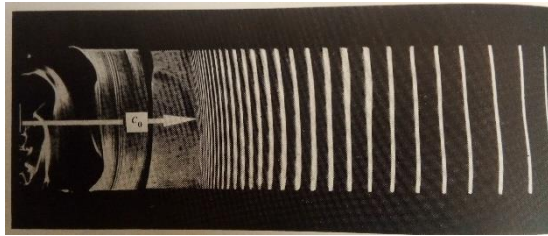


Figure 8 : *Micrograph by Kerkhof and Richter [23] showing a crack with initial edge length c_0 moving (from left to right) with a velocity increasing gradually to reach the terminal velocity. The vertical bright lines are the crack front positions captured at identical time interval. The terminal velocity corresponds to equal distance between the lines at the end right. The specimen length is 180 mm. See [23] for details*

The existence of a terminal velocity for tensile cracks in brittle materials is widely acknowledged [24, 25]. This suggests that the quasi-static configuration, corresponding to small v in spatial region located about c_0 in **Figure 8**, is not an equilibrium one. Subsequent question is: can this terminal velocity be predicted? Interestingly, the answer is yes, from **Figure 4**. The terminal velocity is $\tilde{v}_t^{(e)}$ corresponding to the maximum value $\tilde{G}_{\max}^{(I)}$ of the reduced crack extension force. The condition to be satisfied is $\partial \tilde{G}^{(I)} / \partial \tilde{v}_t = 0$ and this is given by (30). The fact that $\tilde{G}^{(I)}$ increases with crack velocity v from zero up to a maximum has an important implication for a macroscopic crack (by “macroscopic”, we mean that fracture over large distance is under way) under load in an elastic solid. The Griffith condition $G^{(I)} = 2\gamma$ (γ , surface energy) should be applied at the terminal velocity and not at $v = 0$ as commonly proceeded in

laboratory experiments. Under the conditions of **Figure 4**, $\tilde{v}_l^{(e)} \cong 0.52$ and $\tilde{G}_{\max}^{(I)} \cong 1.32$, in isotropic materials with Poisson ratio $\nu = 1/3$. This corresponds to experiments (see [24], for example); above that velocity, crack branching is observed and this is explained by the rapid decrease to zero of the crack extension force $\tilde{G}^{(I)}$. Because the driving force $\tilde{G}^{(I)}$ is becoming small, the moving crack looks for an alternative to propagate rapidly. We now refer to the overview of dynamic fracture mechanics by Freund [25] in support of our findings. In mode II loading, the crack extension force expression $\tilde{G}^{(II)}$ (38) is the same displayed there (see relation (5.3.10) in [25]). The corresponding expression for mode I exhibits the function R_w (see in the text about (36)) in [25], in contrast to our relation (28). However, we have checked that both expressions are identical for small ν . An attempt to derive the terminal velocity expression is presented by Lawn [24]; this makes use of Mott [26] extension of the Griffith concept to dynamic fracture. The estimated value falls well below the Rayleigh wave velocity and closer to our findings. From its maximum value, $\tilde{G}^{(I)}$ decreases continuously to zero at $v = c_t$ (**Figure 4**). This contrasts with many who argue that the theoretical limiting speed of a tensile crack must be the Rayleigh wave speed (see [25, 27], for example). In the transonic velocity regime ($c_t < v < c_l$), the crack functions (35) are identical in form with those of the subsonic regime; however, contrary to the latter where $C_1^{(I)}$ is positive, $C_2^{(I)}$ (or equivalently $1/C_2^{(I)}$) changes sign in the former (**Figure 5**). For $\tilde{v}_l < c_*\sqrt{2}$, $C_2^{(I)}$ is negative. Mathematically, one can transfer the minus sign to the tensile applied stress σ_{22}^a and write, for example,

$$\phi_l(x_1) = \frac{b(-\sigma_{22}^a)}{\pi |C_2^{(I)}|} \sqrt{c^2 - x_1^2}. \tag{42}$$

The corresponding physical interpretation is that over $|x_1| < c$, an ellipse of material has been removed so that under the action of a compressive applied stress ($-\sigma_{22}^a$), the two faces of the elliptical hole close, but remain stress free. In fact, at $t = 0$, just before crack motion, the crack shape is elliptical. The action of the velocity in this region is to close the crack under movement; this suggests that the motion of the crack is inhibited. For $\tilde{v}_l > c_*\sqrt{2}$, $C_2^{(I)}$ becomes positive, suggesting possible motion of the crack.

IV-3. Mode II loaded cracks

Physical quantities associated to the crack are given in (38) in the subsonic speed regime ($v < c_t$), except at the Rayleigh velocity c_R . As can be seen from **Figure 6**, $C_1^{(II)}$ is negative above c_R . A relation like (42) can be written

$$\phi_{II}(x_1) = \frac{b(-\sigma_{21}^a)}{\pi |C_1^{(II)}|} \sqrt{c^2 - x_1^2}. \quad (43)$$

A similar suggestion in discussing (42) is applied here: the motion of the crack is impeded in the velocity interval $c_R < v < c_t$. Rayleigh wave velocity appears to be the limiting speed of a moving crack under mode II loading in the subsonic regime. In the intermediate regime ($c_t < v < c_l$), the crack functions are similar in form to (38) with $C_2^{(II)}$ replacing $C_1^{(II)}$. Because $C_2^{(II)}$ is positive (**Figure 7**), the crack motion is possible.

V - CONCLUSION

An analysis is made of planar cracks located in the Ox_1x_3 – plane with a straight front parallel to x_3 in isotropic materials. The crack fronts travel along x_1 with a constant velocity v under mode I and II loadings. Cracks are represented by a continuous distribution of uniformly moving straight edge dislocations parallel to x_3 with Burgers vectors \vec{b}_J directed along x_1 ($J = II$) or x_2 ($J = I$), according to the loading mode J . Explicit expressions of the elastic fields (displacement and stress) of the crack dislocations are first given for velocities, from zero to values larger than c_l , the velocity of longitudinal sound wave. Then, crack physical quantities are given, namely the dislocation distribution function D_J , the relative displacement ϕ_J of the faces of the crack, the crack-tip stresses and the crack extension force $G^{(J)}$ per unit length of the crack front. These results cover the velocity range $[0, c_l]$. In mode I loading and in the subsonic velocity regime ($v < c_t$, the velocity of transverse sound wave), $G^{(I)}$ increases continuously with v from the value in the static case $G_0^{(I)}$ ($v = 0$) to a maximum $G_{\max}^{(I)} \cong 1.32G_0^{(I)}$ at $v = v^{(e)} \cong 0.52c_t$ (**Figure 4**); then, $G^{(I)}$ decreases rapidly to zero when v tends to c_t . The value $v^{(e)}$ corresponding to the maximum of the crack extension force is identified to the terminal tensile crack velocity, experimentally observed in the fracture of brittle materials. No reference is made to the Rayleigh wave velocity c_R . In the transonic speed regime ($c_t < v < c_l$), the crack characteristic functions (35) are identical in form with those of the subsonic regime. However, for $v < c_t/\sqrt{2}$, it is shown that the faces of the crack,

separated under load before the extension of the crack, close under motion; this indicates that the crack movement is hindered. for $v > c_t\sqrt{2}$, the motion of the crack is possible. In mode II loading and in the subsonic regime ($v < c_t$), $G^{(III)}$ increases continuously with v (when $v < c_R$) from the calculated value in the static case $G_0^{(III)}(v = 0)$; when v approaches c_R , $G^{(III)}$ increases very rapidly (**Figure 6**). Above c_R ($c_R < v < c_t$), the relative displacement of the faces of the crack, formed under load before crack motion, closes in movement; this indicates that crack motion is impeded. The velocity of uniformly moving cracks is limited by the Rayleigh wave velocity. In the intermediate speed regime ($c_t < v < c_l$), the crack characteristic functions are similar in form to (38) with $C_2^{(III)}$ (39) replacing $C_1^{(III)}$ (36). Because $C_2^{(III)}$ is positive (**Figure 7**), the movement of the crack is possible.

REFERENCES

- [1] - P.N.B. ANONGBA, *Physica Stat. Sol. B*, 194 (1996) 443 - 452
- [2] - P.N.B. ANONGBA, *Int. J. Fract.*, 124 (2003) 17 - 31
- [3] - P.N.B. ANONGBA and V. VITEK, *Int. J. Fract.*, 124 (2003) 1 - 15
- [4] - P.N.B. ANONGBA, *Rev. Ivoir. Sci. Technol.*, 14 (2009) 55 - 86
- [5] - P.N.B. ANONGBA, *Rev. Ivoir. Sci. Technol.*, 16 (2010) 11 - 50
- [6] - P.N.B. ANONGBA, *Rev. Ivoir. Sci. Technol.*, 20 (2012) 1 - 23
- [7] - P.N.B. ANONGBA, *Rev. Ivoir. Sci. Technol.*, 30 (2017) 37 - 57
- [8] - P.N.B. ANONGBA, *Rev. Ivoir. Sci. Technol.*, 23 (2014) 54 - 71
- [9] - P.N.B. ANONGBA, *Rev. Ivoir. Sci. Technol.*, 24 (2014) 26 - 44
- [10] - P.N.B. ANONGBA, *Rev. Ivoir. Sci. Technol.*, 32 (2018) 10 - 47
- [11] - P.N.B. ANONGBA, J. BONNEVILLE and A. JOULAIN, *Rev. Ivoir. Sci. Technol.*, 17 (2011) 37 - 53
- [12] - P.N.B. ANONGBA, *Rev. Ivoir. Sci. Technol.*, 26 (2015) 76 - 90
- [13] - P.N.B. ANONGBA, *Rev. Ivoir. Sci. Technol.*, 34 (2019) 25 - 43
- [14] - P.N.B. ANONGBA, *Physica Stat. Sol. B*, 190 (1995) 135 - 149
- [15] - P.N.B. ANONGBA, *Rev. Ivoir. Sci. Technol.*, 26 (2015) 36 - 75
- [16] - P.N.B. ANONGBA, *Rev. Ivoir. Sci. Technol.*, 28 (2016) 24 - 59
- [17] - P.N.B. ANONGBA, *Rev. Ivoir. Sci. Technol.*, 30 (2017) 1 - 36
- [18] - T. MURA, In: "Advances in Materials Research" (Edited by H. Herman), Interscience Publications, Vol. 3, (1968) 1 - 108
- [19] - T. MURA, "Micromechanics of defects in Solids", Martinus Nijhoff Publishers, Dordrecht, (1987)
- [20] - B. A. BILBY and J. D. ESHELBY, In: "Fracture", Ed. Academic Press (H. Liebowitz), New York, Vol. 1, (1968) 99 - 182
- [21] - L. D. LANDAU and E. M. LIFSHITZ, "Theory of Elasticity (3rd ed.)", Pergamon Press, Oxford, (1986)
- [22] - J. D. ESHELBY, In: "Solids State Physics 3", Ed. Academic Press (F. Seitz and D. Turnbull), (1956) 79 - 144

- [23] - F. KERKHOF and H. RICHTER, Second Internat. Conference on Fracture, Brighton. Chapman and Hall, London, paper, 40 (1969)
- [24] - B. LAWN, "Fracture of Brittle Solids 2nd Edition", Cambridge University Press, New York, (1993)
- [25] - L. B. FREUND, "Dynamic Fracture Mechanics", Cambridge University Press, New York, (1990)
- [26] - N. F. MOTT, *Engineering*, 165 (1948) 16 - 18
- [27] - K. B. BROBERG, "Cracks and Fracture", Academic Press, San Diego, (1999)